

Acceleration of the Universe driven by the Casimir force

Marek Szydlowski*

*Astronomical Observatory, Jagiellonian University,
Orla 171, 30-244 Kraków, Poland and
Complex Systems Research Centre, Jagiellonian University,
Reymonta 4, 30-059 Kraków, Poland*

Włodzimierz Godłowski†

*Astronomical Observatory, Jagiellonian University,
Orla 171, 30-244 Kraków, Poland*

We investigate an evolutionary scenario of the FRW universe with the Casimir energy scaling like $(-)(1+z)^4$. The Casimir effect is used to explain the vacuum energy differences (its value measured from astrophysics is so small compared to value obtained from quantum field theory calculations). The dynamics of the FRW model is represented in terms of a two-dimensional dynamical system to show all evolutionary paths of this model in the phase space for all admissible initial conditions. We find also an exact solution for non flat evolutionary paths of Universe driven by the Casimir effect. The main difference between the FRW model with the Casimir force and the Λ CDM model is that their generic solutions are a set of evolutionary paths with a bounce solution and an initial singularity, respectively. The evolutionary scenario are tested by using the SNIa data, FRIIb radiogalaxies, baryon oscillation peak and CMB observation. We compare the power of explanation of the model considered and the Λ CDM model using the Bayesian information criterion and Bayesian factor. Our investigation of the information criteria of model selection showed the preference of the Λ CDM model over the model considered. However the presence of negative like the radiation term can remove a tension between the theoretical and observed primordial ^4He and D abundance.

PACS numbers: 98.80.Jk, 04.20.-q

I. INTRODUCTION

The recent astronomical observations like SNIa [1, 2], WMAP [3] indicate that the current Universe is in an accelerating phase of its expansion. While there are many different explanations of this phenomenon [4] the most straightforward one is that the Universe acceleration is due to the presence of a dark energy component comprising more than 70% of the energy of the Universe. Within this class of models the simplest candidate for dark energy is the phenomenological cosmological constant interpreted as vacuum energy [5]. Unfortunately a simple estimation from quantum field theory gives that vacuum energy is larger than what we observe by a factor of the order 10^{120} . This discrepancy is called the cosmological constant problem and we are looking for some physical process which works to set vacuum energy precisely to zero. The Casimir force which is the manifestation of the quantum fluctuation can offer some mechanism to suppress the cosmological constant interpreted as vacuum energy to the value close to zero at the present epoch [6, 7, 8, 9]. In this context the Casimir effect [10] seems to be relevant because it teaches us how vacuum energy contributes to the cosmological constant. Many other authors (see for example [11]) argue that the Casimir effect is responsible for the vacuum energy differences between the value predicted by the quantum field theory and obtained from observations. Recently Antoniadis et al. [7] has suggested an important role of the Casimir effects in dark energy problem.

Ishak [6] pointed out the relevance of experiments at the interface of astrophysics and quantum field, focusing on the Casimir effects. Nontrivial topology of the Universe [12] was the motivations of these investigations in the cosmological context. Zeldovich and Starobinsky [13] investigated the simple closed FRW models equipped in a 3-torus topology. The Casimir energy has been also studied in the context of compactification of extra-dimensions as an effective mechanism of dimensional reduction [14, 15, 16]. It is worthy to mention that the Casimir type of contribution which arises from the tachyon condensation is also possible [17].

For example in a toroidal model with the compactification scale L , one typically obtains a Casimir contribution $\rho = \langle T_0^0 \rangle = -\frac{\alpha}{L^4} a^4$ [18] (see also [19]) with the scale factor a and the constant term α which depends on the nature

*Electronic address: szydlo@oa.uj.edu.pl

†Electronic address: godlows@oa.uj.edu.pl

and the number of matter fields. The analogous result was obtained by Wreszinski who used the “cosmic box” idea of Harrison [20] to explain why the cosmological constant assumes an absurdly small value of energy density. For this aim local theory of the Casimir effect was applied to the Universe as a whole. The case of massless scalar field with no potential was also investigated in the cosmological context by Hardeiro and Sampaio [21]. The authors study backreaction of the metric on quantum effects in terms of fluid with Casimir energy $\rho_{\text{Cas}} = \alpha/a^4$, pressure $p_{\text{Cas}} = \alpha/3a^4$ and the sign of α for a massless scalar as a function of coupling ξ . The constant α changes the sign corresponds to a theory where the renormalized energy vanishes in the Einstein static universe. This critical value is $\xi_{\text{crit}} \simeq 0.05391$.

The massless conformally coupled scalar field as well as the electromagnetic field and the massless Dirac field on the background of the Einstein static universe (or equivalently quantum effects calculated in the adiabatic approximations which can be justified by the fact that characteristic time scale of quantum process is smaller than a scale of time evolution) were considered in Refs. [22, 23, 24]. In all cases the Casimir energy is of the form α/a^4 ; when α is positive, than Casimir energy is an attractive force, while in an opposite case is repulsive [13]. In the latter case Zeldovich and Starobinski [13] suggested that the scalar field could drive inflation in a flat universe with a nontrivial-toroidal topology. It is interesting that a dynamical effect of the Casimir force is dynamically equivalent to effects of loop quantum gravity effects [25].

The FRW model with the Casimir type force contains a term which scales like negative radiation $(-)(1+z)^4$. One should note that there are different interpretations of the presence of such a term: a cosmological model with global rotation, the Friedmann-Robertson-Walker (FRW) model in the Randall-Sundrum scenario with dark radiation, the FRW universe filled with a massless scalar field in a quantum regime or the FRW model in a semi-classical approximation of loop quantum gravity [26, 27], however in the present paper the FRW universe filled with a massless scalar field in a quantum regime (Casimir effect) is of our special interest.

Our paper is organized as follows. In section II we provide some useful dynamical background for further presentation. In section III we discuss observational constraints on the parameters of model under consideration. We complete the paper by Appendix in which we present an exact solution in the bouncing cosmology with the Casimir effect.

II. DYNAMICS OF THE FRW MODEL WITH THE CASIMIR DARK RADIATION TERM

In this section we investigate dynamical effects of the Casimir force which phenomenologically can be modelled by the Casimir energy $\rho_{\text{Cas}} \propto (-)a^{-4}$, where a is the scale factor. It can be shown that dynamical low temperature quantum effects of a scalar field can be modelled in terms of such perfect fluid [14, 15, 16]. It is useful to investigate the FRW dynamics with the cosmological constant and the Casimir force using dynamical system methods. The main advantage of this tool is possibility of investigations of all evolutionary path for all admissible initial conditions. The main feature of cosmological models with the Casimir force is the presence of the bounce instead of the standard initial singularity. It is worth mentioning that it is not possible by using a geometrical test (basing on null geodesics) to separate an individual Casimir component from all scaling in an analogous way, like $(1+z)^4$ [26, 27].

We consider the FRW model filled by a perfect fluid with energy ρ and pressure p . Then the evolution of the scale factor a can be described by the simple acceleration equation

$$\frac{\ddot{a}}{a} = -\frac{1}{6}(\rho + 3p), \quad (1)$$

where ρ and p are function only the scale factor. It is convenient to represent equation (1) in term of dimensionless variable $x = \frac{a}{a_0}$, where a_0 is the value of the scale factor at the present epoch in the form analogous to the Newtonian equation of motion, i.e.

$$\ddot{x} = -\frac{\partial V}{\partial x}(x), \quad (2)$$

where $V(x)$ is the potential function and overdot here denotes the differentiation with respect to the rescaled cosmological time t such that $t \rightarrow \tau: |H_0|dt = d\tau$, H_0 is the present value of the Hubble function.

The Newtonian equation of motion (2) are equivalent to two-dimensional dynamical system of a Newtonian type

$$\dot{x} = y, \quad \dot{y} = -\frac{\partial V}{\partial x}. \quad (3)$$

Therefore, admissible critical points $y_0 = 0, \frac{\partial V}{\partial x}|_{x_0} = 0$ can be only saddles or centers.

Let us consider the Universe with the cosmological constant ($p_\Lambda = -\rho_\Lambda, \rho_\Lambda = \Lambda$) filled by standard matter in which there are present the Casimir effect modelled as the phenomological fluid scaling like $\rho_{\text{Cas}} \propto (-)a^4$. The assumed

negative sign of energy ρ_{Cas} denote that the Casimir force is attractive. The potential is

$$V(x) = -\frac{1}{2}(\Omega_{\Lambda,0}x^2 - \Omega_{k,0} + \Omega_{m,0}x^{-1} + \Omega_{\text{Cas},0}x^{-2}), \quad (4)$$

where τ is new time parameter proportional to the original cosmological time t such that $t \rightarrow \tau: (H_0)dt = d\tau$; $x = a/a_0$ is a dimensionless scale factor expressed in the units of its present value a_0 , $\Omega_{i,0}$ are the density parameters for matter ($i = m$), the Casimir contribution ($i = \text{Cas}$), the cosmological constant ($i = \Lambda$) and the curvature k (the curvature index $k = 0, \pm 1$).

Equation (4) admits the first integral

$$\frac{(x')^2}{2} + V(x) = E \equiv 0 \quad (5)$$

which has a simple interpretation of conservation energy. The universe is presently ($x = 1$) accelerating if $V(x)$ is a decreasing function of its argument x : $(\frac{dV}{dx})_{x=1} < 0$.

From equation (5) we obtain at the present epoch the constraint $V(x = 1) = -\frac{1}{2}$ or

$$\sum_i \Omega_{i,0} = 1. \quad (6)$$

From equation (4) we obtain that negative values of α as well as the positive cosmological constant give rise to acceleration of the Universe. Because of constraint (5) the motion of the system takes place in a domain $\mathcal{D}_0 = \{x: V(x) \leq 0\}$ of the configuration space.

If we shift the curvature term $-\frac{1}{2}\Omega_{k,0}$ on the right hand side of (5) then system (4) can be considered on the constant energy level $E = -\frac{1}{2}\Omega_{k,0}$ parametrized by the curvature constant. The phase space (x, x') of all trajectories for all admissible initial conditions is divided by trajectory of the flat models $\Omega_{k,0} = 0$. Closed models ($\Omega_{k,0} < 0$) are situated inside this characteristic curve and open models ($\Omega_{k,0} > 0$) outside.

The phase portraits together with the potential function (4) are shown in Fig. 1 and Fig. 2 for $\alpha < 0$ and $\alpha > 0$, respectively. From the phase portrait in Fig. 2 (for $\alpha < 0$, $\rho_{\text{Cas}} = \alpha a^{-4}$) we can observe that the initial singularity characteristic for the case of $\alpha > 0$ is replaced by a bounce. To have a bounce, there must be some time at which the size of the universe (or the scale factor) assumes a minimum: $\dot{a}(t_0) = 0$. Moreover $\ddot{a}(t_0) \geq 0$ is required. The sufficient condition for the origin of the FRW universe from a bounce was formulated by Molina-Paris and Visser [28]. From the point of view of the structural stability notion there is the main difference between phase portraits in Fig. 1 and Fig. 2. The phase portrait for the Λ CDM model is structurally stable. This means that small perturbation of right-hand sides does not disturb the phase portrait. In contrast to Fig. 1 the phase portrait in Fig. 2, is structurally unstable due to presence of centre on x -axis. Following the Peixoto theorem the Λ CDM dynamical system is generic in the class of all planar dynamical systems and bouncing cosmological models are exceptional because do not form such open dense subsets. The type of a critical point is determined by eigenvalues of the linearization matrix calculated at the critical point. This equation assumes the form $\lambda^2 + \frac{\partial^2 V}{\partial x^2} \Big|_{x=x_0} = 0$. Therefore the bounce representing by a centre is present on the phase portrait if $V_{xx}(x_0) > 0$, where $V_x(x_0) = 0$, x_0 is the critical point geometrically it means that $V(x)$ function has minimum in x_0 .

Note that all models on the phase portraits behaves reflectional symmetry $x \rightarrow (-)x$, $x' \rightarrow (-)x'$. During the bounce the SEC (strong energy condition) violation is necessary.

For present acceleration of the universe it is required

$$-\Omega_{m,0} - 2\Omega_{\text{Cas},0} + \Omega_{\Lambda,0} > 0. \quad (7)$$

Therefore if $\Lambda = 0$ the Casimir force must be sufficiently large

$$(|\Omega_{\text{Cas},0}| + \Omega_{\Lambda,0}) > \frac{\Omega_{m,0}}{2} \quad (8)$$

The bouncing cosmology is following of Barrow's reincarnation of ancient fascination of cyclicity and realization myth of the "eternal return" [29]. While the classical bounces are generated by fields endowed with negative energy, the quantum gravity effects in semi-classical approximation invoked to justify the bounce [30] generated by some quantum corrections terms. Also possibility that a contracting braneworld model experiences a bounce instead ever reaching a singularity is addressed by Shtanov and Sahni [31, 32, 33, 34].

Recently bouncing cosmology has been analyzed in details in [35]. It was also demonstrated that the probability of a bounce is close to unity for models of $f(R)$ nonlinear gravity [36, 37, 38].

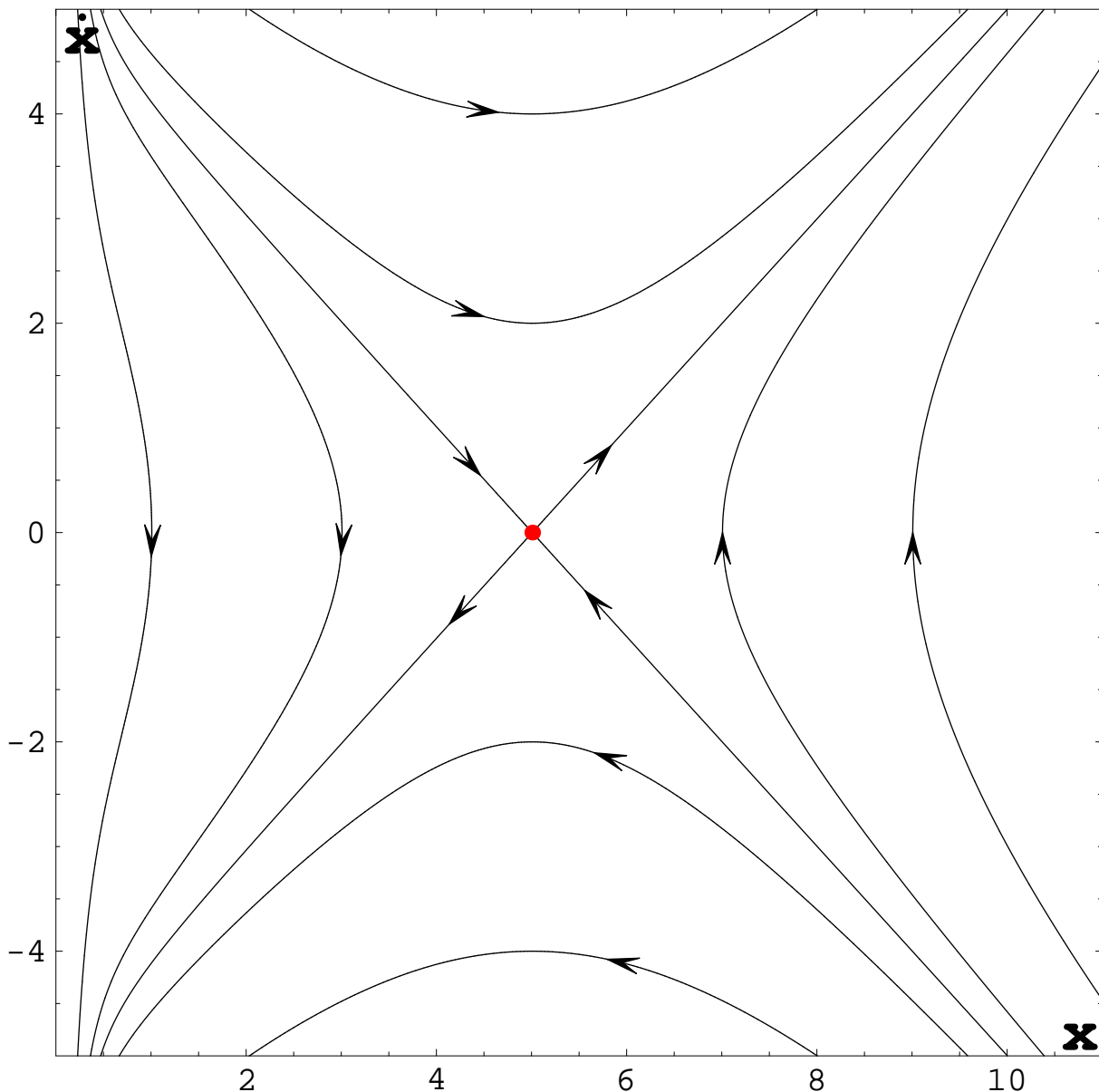


FIG. 1: Phase portrait for the FRW model with $\alpha > 0$ (usual radiation) and the cosmological constant Λ (positive). There are three different types of evolution oscillating, loitering and bouncing. The trajectory $k = 0$ of the flat model separates all the evolutionary paths of closed and open models.

III. TOWARD TESTING BOUNCING COSMOLOGY CAUSED BY $(-)(1+z)^4$ TERM

It is very interesting to test cosmological models against observations. One of the most popular test used the SNIa data. This test is based on the luminosity distance d_L of the supernovae Ia as a function of redshift [1]. The observations of the type Ia distant supernova suggest that the present Universe is accelerating [1, 2, 39, 40]. Every year new SNIa enlarge the available data by more distant objects and lower systematic errors. Our work is based on two samples: Riess et al. [39] “Gold” sample of 157 SNIa and Astier et al. [41] sample of supernovae, based on 71 high redshifted SNIa discovered during the first year of the 5-year Supernovae Legacy Survey. We used this sample because we would like to easily compare the result obtained in present paper with that obtained, with using of different method, in our previous paper [26].

One should note that for the distant SNIa, we directly observe their apparent magnitude m and redshift z . The

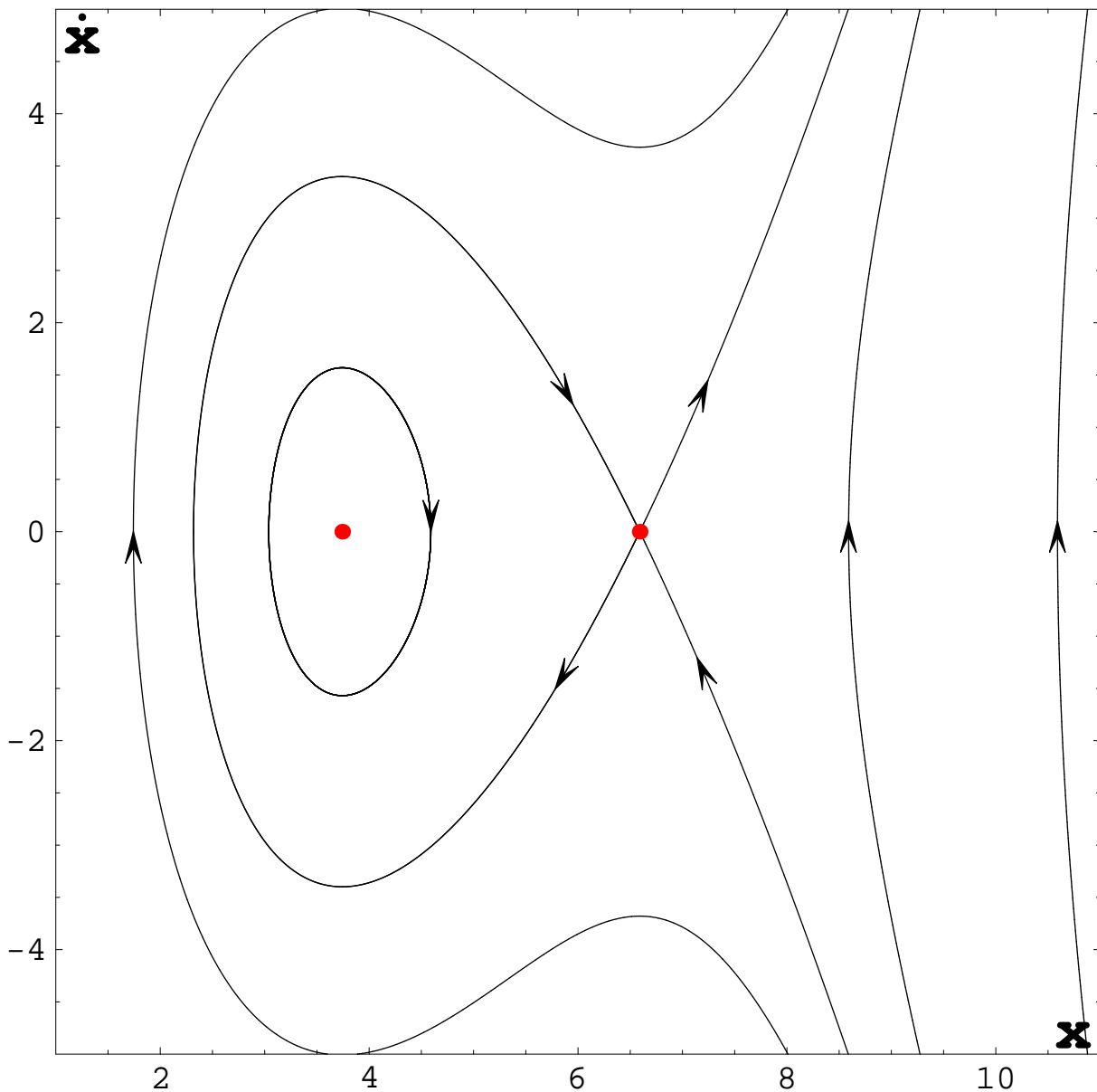


FIG. 2: Phase portrait for the FRW model with the repulsive Casimir force ($\alpha < 0$). All models are undergoing a bounce instead of an initial singularity replaced by the critical point $(x, \dot{x}) = (0, \infty)$ like in Fig. 1. In the phase portrait there are present two types of static critical points center and saddle point like in Fig. 1. Note that bounce appears to be possible in open flat and closed cosmologies. The phase portrait is structurally unstable in contrast to the Λ CDM model represented in Fig. 1.

absolute magnitude \mathcal{M} of the supernovae is related to its absolute luminosity L . We have the following relation between distance modulus μ , the luminosity distance d_L , the observed magnitude m and the absolute magnitude M :

$$\mu \equiv m - M = 5 \log_{10} d_L + 25 = 5 \log_{10} D_L + \mathcal{M} \quad (9)$$

where $D_L = H_0 d_L$ and $\mathcal{M} = -5 \log_{10} H_0 + 25$. The luminosity distance of a supernova is the function of cosmological parameters and redshift

$$d_L(z) = (1+z) \frac{c}{H_0} \frac{1}{\sqrt{|\Omega_{k,0}|}} \mathcal{F} \left(H_0 \sqrt{|\Omega_{k,0}|} \int_0^z \frac{dz'}{H(z')} \right) \quad (10)$$

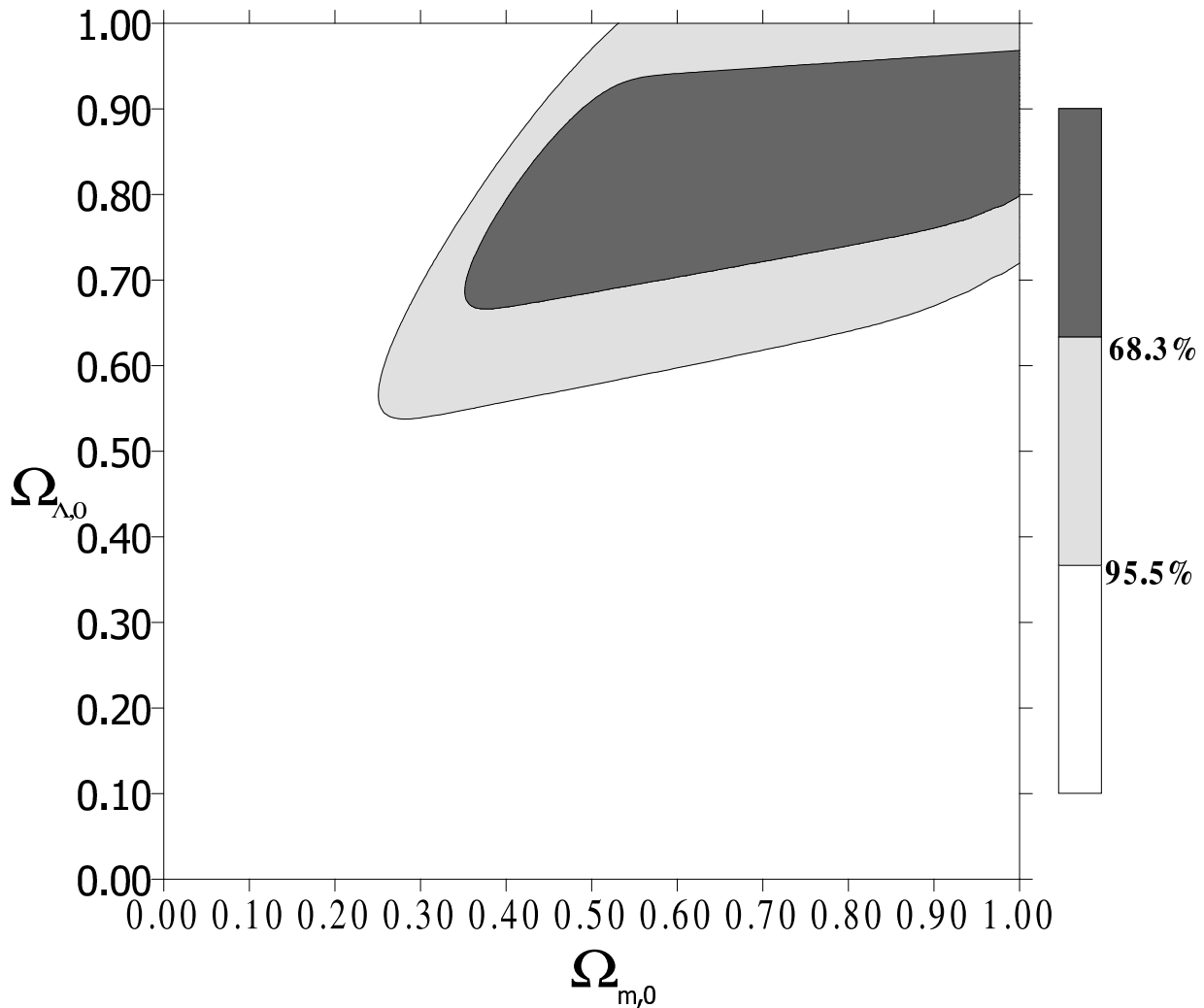


FIG. 3: The 68.3% and 95.4% confidence levels obtained from combined analysis SN+RG) on the $(\Omega_{m,0}, \Omega_{\Lambda,0})$ plane.

where

$$\left(\frac{H}{H_0}\right)^2 = \Omega_{m,0}(1+z)^3 + \Omega_{k,0}(1+z)^4 + \Omega_{r,0}(1+z)^4 + \Omega_{dr,0}(1+z)^4 + \Omega_{\Lambda,0}, \quad (11)$$

$\Omega_{k,0} = -\frac{k}{H_0^2}$ and $\mathcal{F}(x) \equiv (\sinh(x), x, \sin(x))$ for $k < 0, k = 0, k > 0$, respectively. We assumed $\Omega_{r,0} = \Omega_{\gamma,0} + \Omega_{\nu,0} = 2.48h^{-2} \times 10^{-5} + 1.7h^{-2} \times 10^{-5} \simeq 0.0001$ [42].

Substituting (10) back into equations (9) provides us with an effective tool (the Hubble diagram) to test cosmological models and to constrain their parameters. Assuming that supernovae measurements come with uncorrelated Gaussian errors, one can determine the likelihood function \mathcal{L} from chi-square statistic $\mathcal{L} \propto \exp(-\chi^2/2)$, where

$$\chi^2 = \sum_i \frac{(\mu_i^{\text{theor}} - \mu_i^{\text{obs}})^2}{\sigma_i^2}. \quad (12)$$

The probability density function (PDF) of cosmological parameters [1] can be derived from Bayes' theorem. Therefore, one can estimate model parameters by using a minimization procedure. It is based on the likelihood function as well as on the best fit method minimizing χ^2 . Constraints for the cosmological parameters, can be obtain by minimizing the following likelihood function $\mathcal{L} \propto \exp(-\chi^2/2)$.

Daly and Djorgovski [43] (see also [26, 27, 44, 45]) suggested to include in the analysis not only supernovae but also

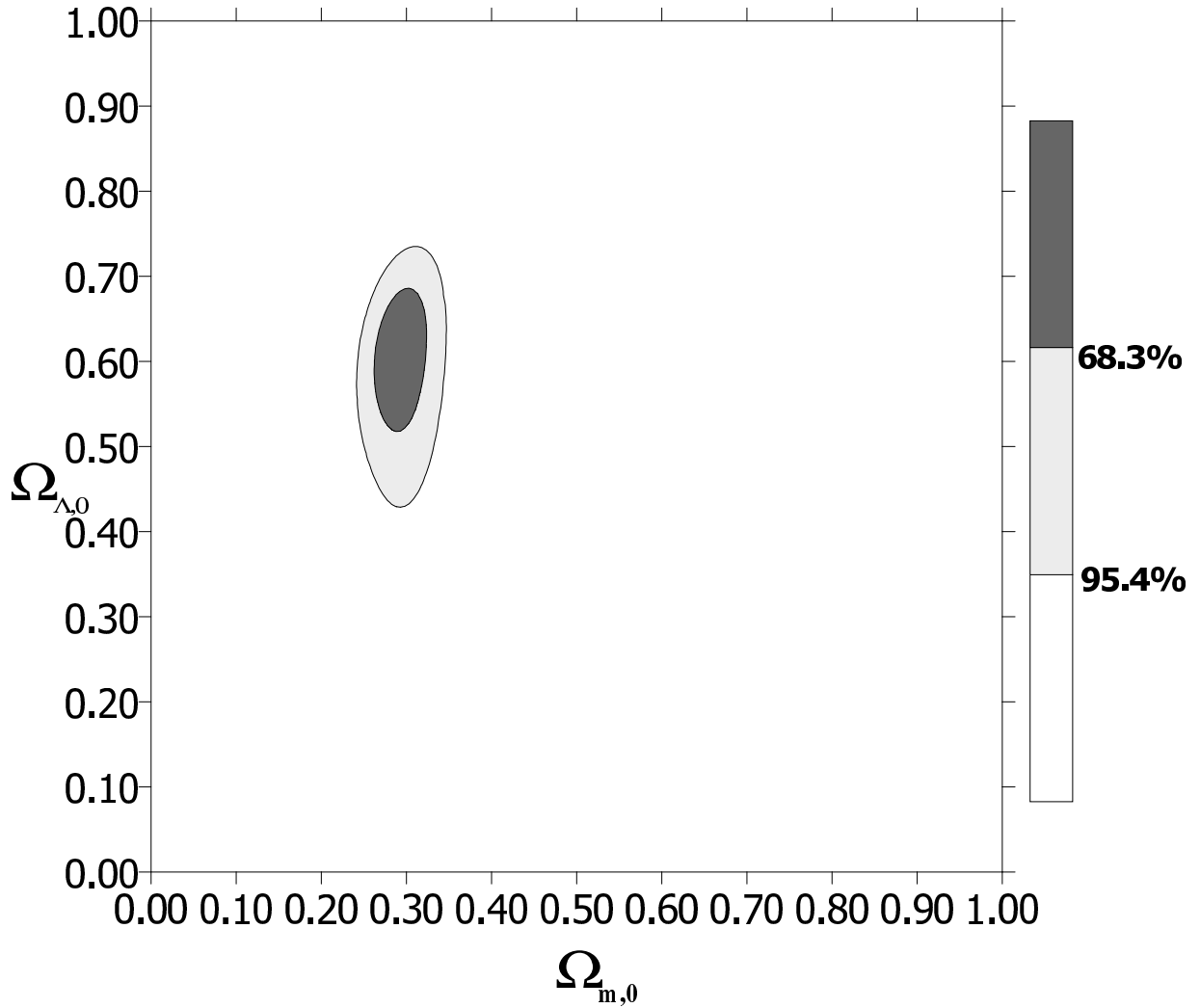


FIG. 4: The 68.3% and 95.4% confidence levels obtained from combined analysis SN+RG+BOP) on the $(\Omega_{m,0}, \Omega_{\Lambda,0})$ plane.

radio galaxies. In such a case, it is useful to use the coordinate distance defined as [46]

$$y(z) = \frac{H_0 d_L(z)}{c(1+z)}. \quad (13)$$

In such a case we can determinate likelihood function $\mathcal{L} \propto \exp(-\chi^2/2)$, where

$$\chi^2 = \sum_i \left(\frac{y_i^{\text{obs}} - y_i^{\text{th}}}{\sigma_i(y_i)} \right)^2 \quad (14)$$

To analyse SNIa data and FRIIb data in the unique way it is useful analyses for both sets of data coordinate distance $y(z)$. Daly and Djorgovski [47] compiled a sample comprising the data on $y(z)$ for 157 SNIa in the Riess et al. [39] Gold dataset and 20 FRIIb radio galaxies. In our data sets we also include 115 SNIa compiled by Astier et al. [41]. In our previous paper [26] there are more details on the computation of $y(z)$ and $\sigma_i(y_i)$ for these samples.

In Fig. 3 we present the 68.3% and 95.4% confidence levels obtained from combined analysis SNIa and FRIIb on the plane $(\Omega_{m,0}, \Omega_{\Lambda,0})$.

We also include to our analysis the baryon oscillation peaks (BOP) detected in the Sloan Digital Sky Survey (SDSS) luminous red galaxies [48]. They found that the value A is

$$A \equiv \frac{\sqrt{\Omega_{m,0}}}{E(z_1)^{\frac{1}{3}}} \left(\frac{1}{z_1 \sqrt{|\Omega_{k,0}|}} \mathcal{F} \left(\sqrt{|\Omega_{k,0}|} \int_0^{z_1} \frac{dz}{E(z)} \right) \right)^{\frac{2}{3}} = 0.469 \pm 0.017 \quad (15)$$

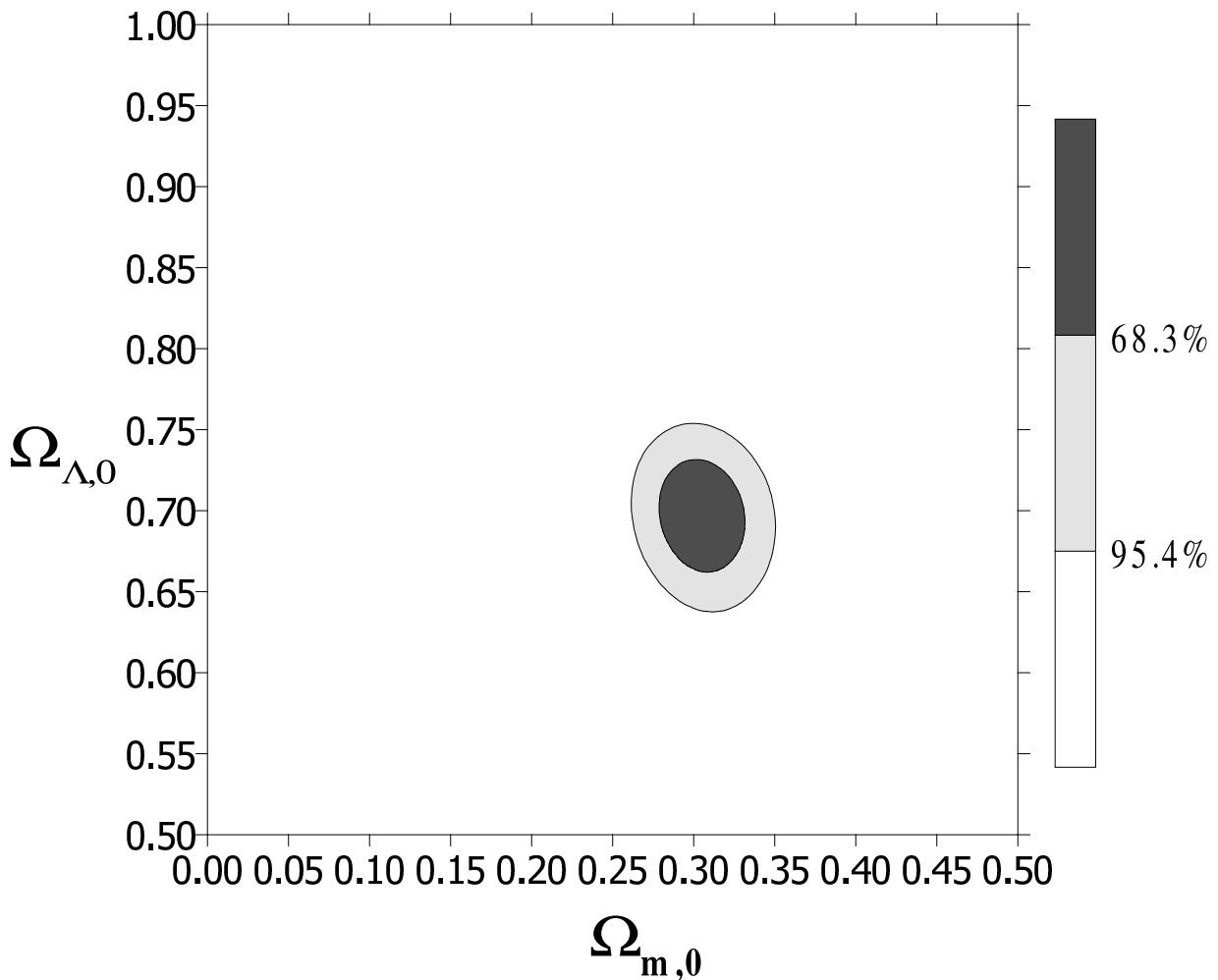


FIG. 5: The 68.3% and 95.4% confidence levels obtained from combined analysis SN+RG+BOP+CMB) on the $(\Omega_{m,0}, \Omega_{\Lambda,0})$ plane.

where $E(z) \equiv H(z)/H_0$ and $z_1 = 0.35$. The quoted uncertainty corresponds to one standard deviation, where a Gaussian probability distribution has been assumed. These constraints could also be used for fitting cosmological parameters [41, 49]. In such a case we determinate the likelihood function $\mathcal{L} \propto \exp\left[-\left(\frac{A^{\text{mod}} - 0.469}{0.017}\right)^2 / 2\right]$.

Another constraint which we also include in our analysis is the so called the (CMBR) “shift parameter” [50]

$$R \equiv \sqrt{\Omega_{m,0}} y(z_{\text{ISS}}) = \sqrt{\frac{\Omega_{m,0}}{|\Omega_{k,0}|}} \mathcal{F}\left(\sqrt{|\Omega_{k,0}|} \int_0^{z_{\text{ISS}}} \frac{dz}{E(z)}\right) = 1.716 \pm 0.062$$

which leads to the likelihood function $\mathcal{L} \propto \exp\left(-\left(\frac{R^{\text{mod}} - 1.716}{0.062}\right)^2 / 2\right)$.

In Fig. 4 and Fig. 5 we present confidence levels obtained from the analysis of SNIa, FRIIb and BOP or BOP and CMB shift, respectively. One should note that when we are interested in constraining a particular model parameter, the likelihood function marginalized over the remaining parameters of the model should be considered [51].

From our combined analysis (SN+RG+SDSS+CMBR) we obtain as the best fit a flat (or nearly flat universe) with $\Omega_{m,0} \simeq 0.3$, and $\Omega_{\Lambda,0} \simeq 0.7$. For the dark radiation term, we obtain the stringent bound $\Omega_{R,0} = \Omega_{r,0} - |\Omega_{\text{dr},0}| > -0.00025$ at the 95% confidence level where $\Omega_{\text{dr},0}$ is negative. It leads for the limit on dark radiation $|\Omega_{\text{dr},0}| < 0.00035$. This results mean that null value of dark radiation term is preferred ($\Omega_{\text{dr},0} = 0$), however the small negative contribution of dark radiation is also available. Our results shows that in the present epoch contribution of the dark radiation, if it exist, is small and gives only small corrections to the Λ CDM model in the low redshift.

Our result is in agreement with the result of our previous paper [26] where in the combined analysis based in a pseudo- χ^2 merit function [51]: we obtain as the best fit a flat universe with $\Omega_{m,0} = 0.3$, $\Omega_{dr,0} = 0$ and $\Omega_{\Lambda,0} = 0.7$. For the dark radiation term, we obtain the stringent bound $|\Omega_{dr,0}| < 0.00035$ at the 95% confidence level ($|\Omega_{dr,0}| < 0.00026$ at the 68.3% confidence level).

Please also note that if $\Omega_{R,0} = \Omega_{r,0} - |\Omega_{dr,0}| < 0$, then we obtain a bouncing scenario [28, 35, 52] instead of a big bang. For $\Omega_{m,0} = 0.3$, $\Omega_{dr,0} = -0.00035$ and $h = 0.65$ bounces ($H^2 = 0$) appear for $z \simeq 1200$. In this case, the BBN epoch never occurs and all BBN predictions would be lost.

We use the Akaike information criterion (AIC) [53], the Bayesian information criterion (BIC) [54] as well as the Bayes factor to select model parameters providing the preferred fit to data. The information criteria put a threshold which must be exceeded in order to assert an additional parameter to be important in explanation of a phenomenon. The discussion how high this threshold should be caused the appearing of many different criteria. The Akaike and Bayesian information criteria (AIC and BIC) (for review see [55]) are most popular and used in everyday statistical practices. The usefulness of using the information criteria of model selection was recently demonstrated by Liddle [56] and Parkinson et al. [57]. The problem of classification of the cosmological models on the light of the information criteria on the base of the astronomical data was discussed in our previous papers [58, 59, 60, 61, 62, 63].

The AIC is defined in the following way [53]

$$\text{AIC} = -2 \ln \mathcal{L} + 2d \quad (16)$$

where \mathcal{L} is the maximum likelihood and d is a number of the free model parameters. The best model with a parameter set providing the preferred fit to the data is that minimizes the AIC. The BIC introduced by Schwarz [54] is defined as

$$\text{BIC} = -2 \ln \mathcal{L} + d \ln N \quad (17)$$

where N is the number of data points used in the fit. Comparing these criteria, one should note that the AIC tends to favor models with large number of parameters unlike the BIC, because the BIC penalizes additional parameters more strongly. Of course only the relative value between the BIC of different models has statistical significance. The difference of 2 is treated as a positive evidence (and 6 as a strong evidence) against the model with the larger value of the BIC [64, 65]. If we do not find any positive evidence from the information criteria the models are treated as a identical and eventually additional parameters are treated as not significant.

In the Bayesian framework quality of the models can be compared with help of evidence [64, 66]. We can define the a'posterior odds for two models M_i and M_j – the Bayes factor B_{ij} [67]. If we do not favor any model it reduces to the evidence ratio. Schwarz [54] showed that for observations coming from a linear exponential family distribution the asymptotic approximation $N \rightarrow \infty$ the logarithm of evidence is given by

$$\ln E = \ln \mathcal{L} - \frac{d}{2} \ln N + O(1). \quad (18)$$

It is easy to show that in this case we have the simple relation between the Bayes factor and the BIC

$$2 \ln B_{ij} = -(\text{BIC}_i - \text{BIC}_j) \quad (19)$$

If B_{ij} is greater than 3 it is called positive evidence in favor of M_i model, while $B_{ij} > 20$ give strong and $B_{ij} > 150$ very strong evidence in favor of M_i model [62].

Our results are presented in Table I. In our investigations we consider the likelihood function $\mathcal{L} \propto \exp(-\chi^2/2)$ where a pseudo- χ^2 merit function is used [26, 27, 51]:

$$\begin{aligned} \chi^2 = \chi_{\text{SN+RG}}^2 + \chi_{\text{SDSS}}^2 + \chi_{\text{CMBR}}^2 = \\ \sum_i \left(\frac{y_i^{\text{obs}} - y_i^{\text{th}}}{\sigma_i(y_i)} \right)^2 + \left(\frac{A^{\text{mod}} - 0.469}{0.017} \right)^2 + \left(\frac{R^{\text{mod}} - 1.716}{0.062} \right)^2, \end{aligned} \quad (20)$$

where A^{mod} and R^{mod} denote the values of A and R obtained for a particular set of the model parameter.

Our investigations of the information criteria show that the bouncing Λ cold dark matter model (B Λ CDM) with dark energy does not increase the fit significantly. It confirms our conclusion that the dark energy term, if it exists, is small in the present epoch. The Bayes factor also favors the Λ CDM model over the B Λ CDM model with dark energy. Its supports results obtained with help of the AIC and BIC. One should note that because of a non-Gaussian distribution of the a'posteriori PDF function for $\Omega_{R,0}$ the above results obtained with help of the Bayes factor should be treated with caution as only an additional support for results obtained with help of the AIC and BIC.

IV. CONCLUSION

In this paper we analyzed the observational constraints on the $(1+z)^4$ -type contribution in the Friedmann equation. The analysis of SNIa data as well as both SNIa and FRIIb radio galaxies with the constraints coming from baryon oscillation peaks and CMBR "shift parameter" shows that influence of a negative term $-(1+z)^4$ is very weak in the present epoch of the Universe.

The main aim of this paper is investigation of evolutionary paths of the FRW cosmological models with the cosmological constant Λ and the Casimir energy scaling like $-(1+z)^4$. We demonstrate that a bounce is a generic feature of this model. In this scenario an initial singularity is replaced by a bounce. We characterize a full class of all evolutionary paths by using dynamic system methods and we find exact solution. We pointed out the main difference between the Λ CDM model and the $B\Lambda$ CDM model from the view of point structural stability. The two-dimensional case of dynamical system is distinguished by the fact that the Peixoto theorem gave a complete characterization of the structurally stable systems on any compact space, assert that they form open and dense subsets in the space of all dynamical systems on the plane. We conclude that while the Λ CDM models are structurally stable, therefore typical, the $B\Lambda$ CDM models are structurally unstable, therefore exceptional. Of course structurally unstable models may model a realistic physical situation however they require a fine tuning of the model itself (not fine tuning of initial conditions).

We show that there are several interpretations of the $(1+z)^4$ -type contribution and we discussed different proposals for the presence of such a term. Unfortunately, it is not possible, with present kinematic astronomical tests, to determine the energy densities of individual components scales like radiation. However we show that some stringent bounds on the value of this total contribution can be given. The combined analysis of SNIa data and FRIIb radio galaxies, baryon oscillation peaks and CMBR "shift parameter" give rise to the concordance universe model which is almost flat with $\Omega_{m,0} \simeq 0.3$. From the above-mentioned combined analysis, we obtain an constraint for the negative term which scales like total radiation $\Omega_{R,0} > -0.00025$ which leads to bounds on the dark radiation term $\Omega_{dr,0} > -0.00035$ at the 95% confidence level. This is in agreement with result of our previous paper [26] obtained with help of a pseudo- χ^2 merit function.

The investigations of the information criteria show the $B\Lambda$ CDM model with dark energy does not increase the fit significantly. It confirms our conclusion that the dark energy term, if it exists, is small in the present epoch.

In this paper we have especially studied the advance of an initial singularity using back reaction gravity quantum effect at low temperatures (the Casimir effect). The Casimir force arising from the quantum effect of massless scalar field give rise to a $-(1+z)^4$ correction whose effect depends upon the geometry and nontrivial topology of the space. Typically this type of correction is thought to be important at the late time of evolution of the universe. We have shown that the Casimir effect could generically remove the initial singularity which would be replaced by the bounce.

Our analysis of back reaction on quantum effect clearly reflects an important role played by vacuum energy. The basic problem which helps us to understand the dynamics of accelerating universe is how the cosmological constant (geometrical) contributes to the vacuum energy.

Acknowledgements

M. S. was supported by the Marie Curie Actions Transfer of Knowledge project COCOS (contract MTKD-CT-2004-517186). Authors are grateful T. Stachowiak for comments and fruitful discussion. The authors also thank Dr. A. G. Riess, Dr. P. Astier and Dr. R. Daly for the detailed explanation of their data samples.

APPENDIX A: BASIC MODELS WITH THE CASIMIR FORCE.

The Friedmann equation we are dealing with can be reduced so that the right-hand side is a 4th degree polynomial. Such equations have been completely analyzed in [68], so we merely point out which cases of the general classification (by which we will mean the cited paper's content) apply and what additional features arise here.

The equation reads:

$$\left(\frac{dy}{du}\right)^2 = \Omega_{\Lambda,0}y^2 - \Omega_{k,0} + \Omega_{m,0}y^{-1} + \Omega_{r,0}y^{-2} - \Omega_{\omega}y^{-2}. \quad (\text{A1})$$

Analogously to the $\Omega_{R,0}$ in section III we introduce $\Omega_R = \Omega_{r,0} - \Omega_{\omega}$, and change the variables to:

$$y = x, \quad du = x d\tau,$$

TABLE I: The values of AIC and BIC and Bayes factor B_{12} for Λ CDM model and bouncing cosmology model (with dark radiation). The upper section of the table represents the constraint $\Omega_{k,0} = 0$ (flat model).

sample	Λ CDM		BACDM		B_{12}
	AIC	BIC	AIC	BIC	
SN	299.5	303.1	301.5	308.7	16.44
SN+RG	322.4	326.1	324.4	331.8	17.29
SN+RG+SDSS	324.4	328.1	326.4	333.8	17.29
SN+RG+SDSS+CMBR	324.5	328.2	326.5	333.9	17.29
SN	300.0	307.2	302.0	312.8	16.44
SN+RG	323.5	330.9	325.5	336.5	17.29
SN+RG+SDSS	325.1	332.5	327.1	338.1	17.29
SN+RG+SDSS+CMBR	326.5	333.9	328.5	339.5	17.29

the main equation becomes

$$\left(\frac{dx}{d\tau}\right)^2 = \Omega_{\Lambda,0}x^4 - \Omega_{k,0}x^2 + \Omega_{m,0}x + \Omega_R = W(x). \quad (\text{A2})$$

The only new solutions appear, when one considers Ω_ω big enough, for Ω_R to be negative. Otherwise, the solutions is equivalent to that of a model with radiation only. We note that:

$$W(0) = \Omega_R < 0 \quad (\text{A3})$$

applies to all models, restricting the solutions.

The most general form of the solution, satisfying $x(0) = 1$, reads

$$x = 1 + \frac{\wp'(\tau) + \Omega_{\Lambda,0}}{2[\wp(\tau) - \frac{1}{12}(6\Omega_{\Lambda,0} - \Omega_{k,0})]^2 - \frac{1}{2}\Omega_{\Lambda,0}} + \frac{\frac{1}{2}(4\Omega_{\Lambda,0} - 2\Omega_{k,0} + \Omega_{m,0})[\wp(\tau) - \frac{1}{12}(6\Omega_{\Lambda,0} - \Omega_{k,0})]}{2[\wp(\tau) - \frac{1}{12}(6\Omega_{\Lambda,0} - \Omega_{k,0})]^2 - \frac{1}{2}\Omega_{\Lambda,0}}, \quad (\text{A4})$$

with the invariants

$$\begin{aligned} g_2 &= \frac{1}{12}\Omega_{k,0}^2 + \Omega_{\Lambda,0}\Omega_R, \\ g_3 &= \frac{1}{216}\Omega_{k,0}^3 - \frac{1}{16}\Omega_{\Lambda,0}\Omega_{m,0}^2 - \frac{1}{6}\Omega_{\Lambda,0}\Omega_{k,0}\Omega_R. \end{aligned} \quad (\text{A5})$$

and using it, we can also obtain an explicit formula connecting the conformal and cosmological times.

First, we need to investigate the singular points of our solution. As $x(\tau)$ is an elliptic function of order two, there are exactly two poles (provided that $\Omega_{\Lambda,0} \neq 0$). To specify them exactly, we can use the \wp function, together with its derivative

$$\begin{aligned} \wp(\tau_1) &= +\frac{1}{2}\sqrt{\Omega_{\Lambda,0}} + \frac{1}{2}\Omega_{\Lambda,0} - \frac{1}{12}\Omega_{k,0}, & \wp'(\tau_1) &= +\frac{1}{4}\sqrt{\Omega_{\Lambda,0}} + \Omega_{\Lambda,0}, \\ \wp(\tau_2) &= -\frac{1}{2}\sqrt{\Omega_{\Lambda,0}} + \frac{1}{2}\Omega_{\Lambda,0} - \frac{1}{12}\Omega_{k,0}, & \wp'(\tau_2) &= -\frac{1}{4}\sqrt{\Omega_{\Lambda,0}} + \Omega_{\Lambda,0}. \end{aligned} \quad (\text{A6})$$

Relation $du = xd\tau$ then becomes

$$u = \left\{ 1 + \frac{1}{\sqrt{\Omega_{\Lambda,0}}}[\zeta(\tau_1) - \zeta(\tau_2)] \right\} \tau + \frac{1}{\sqrt{\Omega_{\Lambda,0}}} \ln \left[\frac{\sigma(\tau - \tau_1)\sigma(\tau_2)}{\sigma(\tau - \tau_2)\sigma(\tau_1)} \right], \quad (\text{A7})$$

where the constant of integration was chosen so that $u(\tau = 0) = 0$, and ζ and σ are the appropriate Weierstrass functions.

This formula remains true in the degenerate cases as well, with ζ and σ also simplified. In the case of trigonometric/hyperbolic solutions we have

$$\begin{aligned} \zeta(\tau) &= \frac{1}{2} \left[g\tau + \sqrt{6g} \cot\left(\sqrt{\frac{3}{2}g}\tau\right) \right], \\ \sigma(\tau) &= \sqrt{\frac{2}{3g}} e^{\frac{1}{4}g\tau^2} \sin\left(\sqrt{\frac{3}{2}g}\tau\right), \end{aligned} \quad (\text{A8})$$

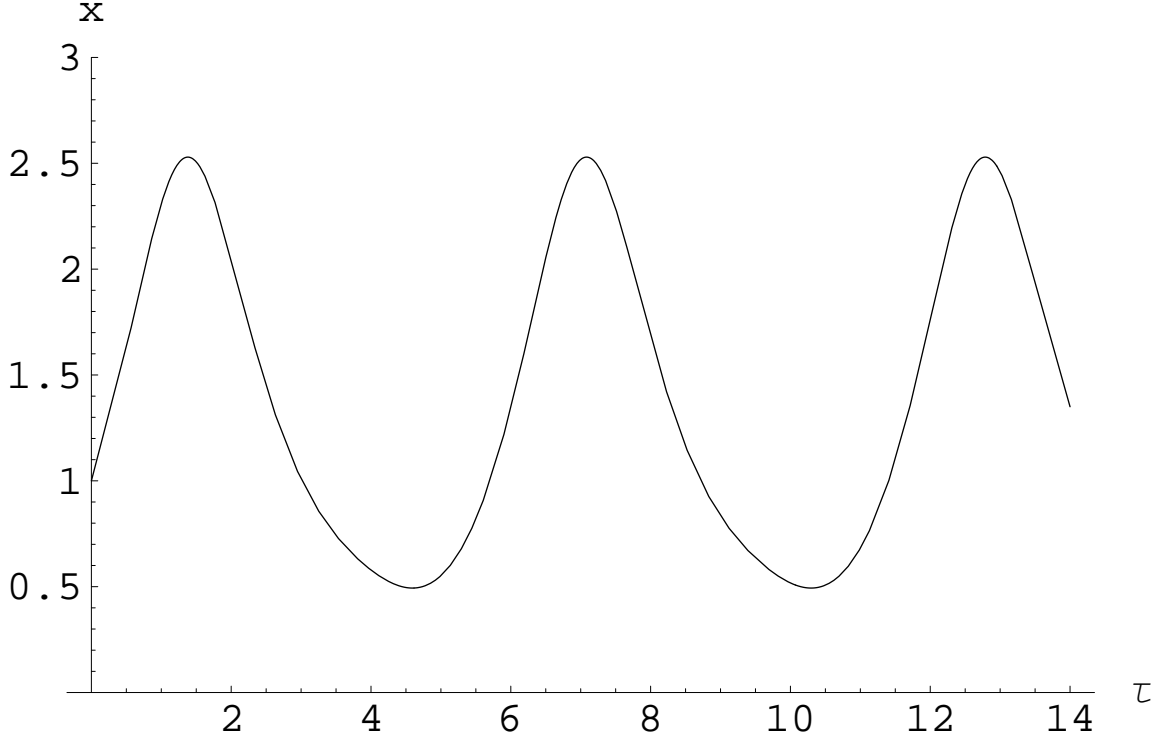


FIG. 6: A generic oscillating solution, which in the considered case is never singular. Scaling from τ to u only results in stretching the time axis.

with $\sqrt{3}g = \pm\sqrt{g_2}$, and for initial conditions chosen as for the general solution.

The two following sections consist of the case by case classification analogous to that of [68] with the quantities $\sigma_i, w_-, x_{+/-/0}$ defined therein.

1. $\Omega_{\Lambda,0} > 0$

1.1. Case $\sigma_6 \neq 0$

Analyzing the behavior of σ_6 , with the possible values of Ω_R and $\Omega_{\Lambda,0}$, we obtain the first important restriction:

$$\Omega_{k,0} \leq 0 \Rightarrow \sigma_6 < 0. \quad (\text{A9})$$

For positive curvature, any sign is possible.

As follows from the general considerations, we have two possibilities: $\sigma_6 > 0$, or $\sigma_6 < 0$. However, the former is limited to the case of four real roots. This happens because we have: $w_- = (2\Omega_{k,0} - \sqrt{\Omega_{k,0}^2 + 12\Omega_R\Omega_{\Lambda,0}})/3$, and by (A9) $\Omega_{k,0} > 0$ while $\Omega_R\Omega_{\Lambda,0} < 0$, causing w_- to be always positive, and making the resolvent cubic admit three solutions.

1.1.1 Four complex roots

This case is impossible, because $\Omega_{\Lambda,0} > 0$ would force w to be positive everywhere.

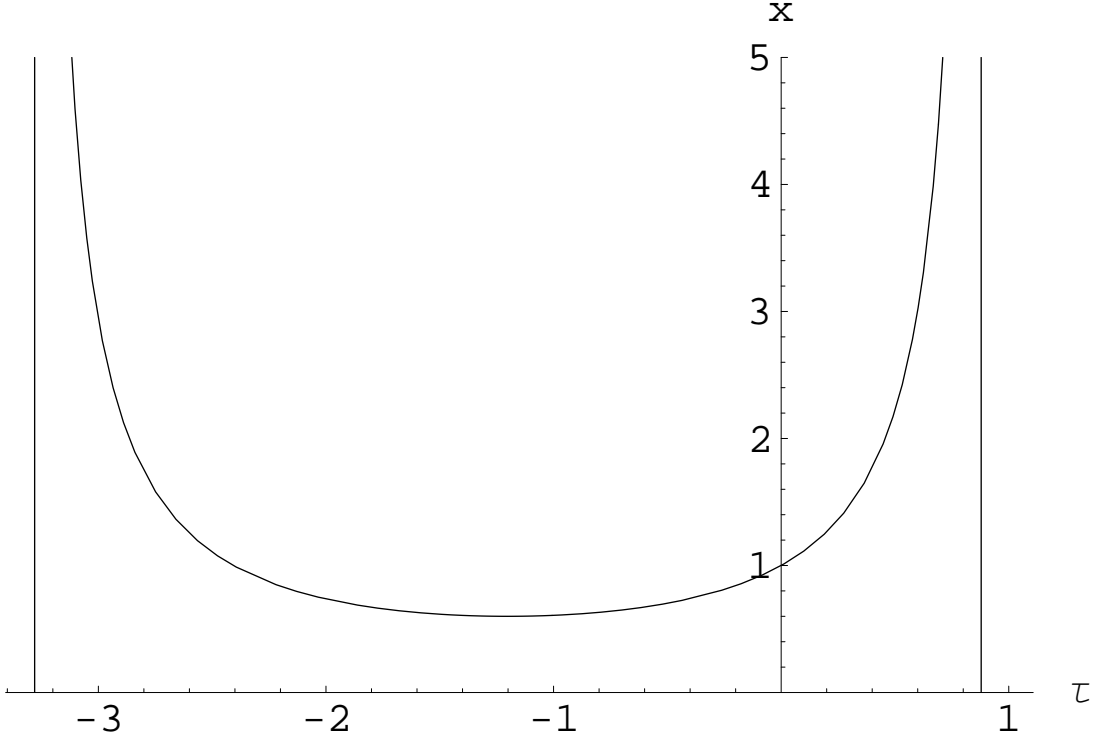


FIG. 7: A typical bounce in finite time τ , corresponding to u changing from $-\infty$ to ∞ .

1.1.2. Four real roots

There are two possibilities here. Either $e_1 < 0 < e_2 < e_3 < e_4$, or $e_1 < e_2 < e_3 < 0 < e_4$. The former admits both the solutions x_0 and x_+ , the latter only x_+ . However, none of them passes through zero, allowing for the particularly interesting non-singular, periodic behavior of x_0 . A typical oscillatory solution is presented in Fig. 6, and the bounce in Fig. 7. Although the latter has a finite time of evolution in τ , this interval is stretched into the whole real line when in the variable u . This happens because the right hand side in (A7) is singular.

1.2. $\sigma_6 = 0$ – one double root

As a consequence of (A9), this, and obviously all the following cases, require *positive curvature*. Also, as in the general classification, we must have:

$$\Omega_{k,0}^2 + 12\Omega_R\Omega_{\Lambda,0} > 0. \quad (\text{A10})$$

As $\sigma_6 = 0$, is effectively an equation of degree two in $\Omega_{\Lambda,0}$ it instantly provides new restrictions. First, for it to have real solutions in $\Omega_{\Lambda,0}$, we must have

$$9\Omega_{m,0}^2 + 32\Omega_{k,0}\Omega_R \geq 0. \quad (\text{A11})$$

and if at least one of the solutions is to be positive, we also need

$$\frac{16\Omega_R\Omega_{k,0}}{\Omega_{m,0}^2} \in \left[-3(3 + \sqrt{3}); -3(3 - \sqrt{3}) \right],$$

finally yielding:

$$\frac{16\Omega_R\Omega_{k,0}}{\Omega_{m,0}^2} \in \left[-\frac{9}{2}; -3(3 - \sqrt{3}) \right]. \quad (\text{A12})$$

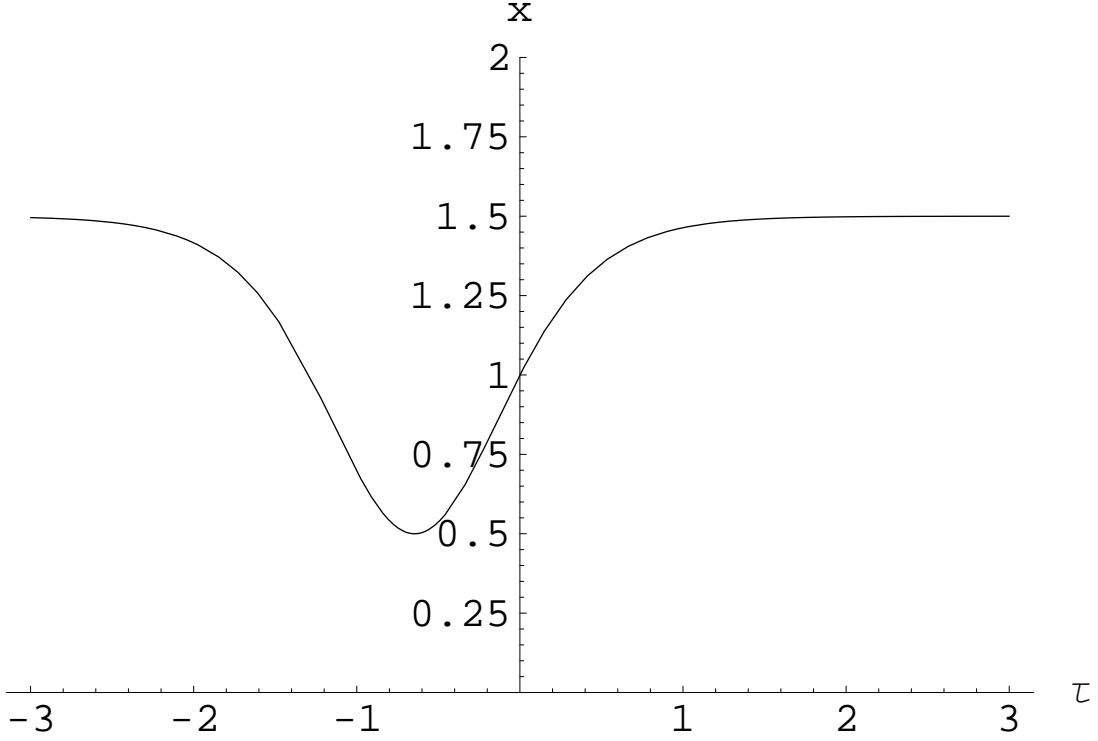


FIG. 8: The quasi-static solution, which stays almost at the same value of the scale factor for most of the time (both τ and u), and undergoes only one short dip.

This also allows us to see that the sign of σ_5 , which is the same as that of the expression $\Omega_{\Lambda,0} - 2k^3 / (9\Omega_{m,0}^2 + 8\Omega_{k,0}\Omega_R)$ in this case, can be both plus and minus. The biggest restriction comes from the inequality (A3), which makes case 1.2.1 impossible. As for 1.2.2, all three subcases might happen. If the double root is the smallest, then we only have the x_{-1} solution (bounce). If it lies between the other roots, we have both the static, stable solution x_0 , and x_+ (bounce). Lastly, if the double root is the biggest, we have both asymptotic branches x_+ and x_{-1} , together with the unstable, static x_0 .

The bouncing solutions are essentially the same as the previous ones (Fig. 7), also with time stretching. As for the asymptotic solutions, we either have a quasi-static evolution x_+ with one minimum, depicted in Fig. 8; or a monotonic expansion/contraction x_{-1} , presented in Fig. 9. The former has an infinite evolution time in both τ and u , and the latter reaches infinite x for finite τ but infinite u .

1.3. $\sigma_6 = \sigma_5 = 0$, $\sigma_4 \neq 0$ – two double roots

Further simplifications require

$$\begin{aligned}\Omega_{\Lambda,0} &= \frac{\Omega_{k,0}^2}{12\Omega_R} \\ \Omega_{m,0} &= \sqrt{-\frac{32}{9}\Omega_{k,0}\Omega_R}.\end{aligned}\tag{A13}$$

However, such a value of $\Omega_{\Lambda,0}$ makes $\sigma_4 = 0$, making this case impossible, and bringing us to the next one.

1.4. $\sigma_6 = \sigma_5 = \sigma_4 = 0$, $\sigma_3 \neq 0$ – one triple root

The so far excluded possibility of $12\Omega_R\Omega_{\Lambda,0} + \Omega_{k,0}^2 = 0$, holds here, and substituting (A13) into σ_3 , we see that further simplification is not possible, as σ_3 is proportional to $\Omega_R^3 \neq 0$. Following the general classification 1.4, we

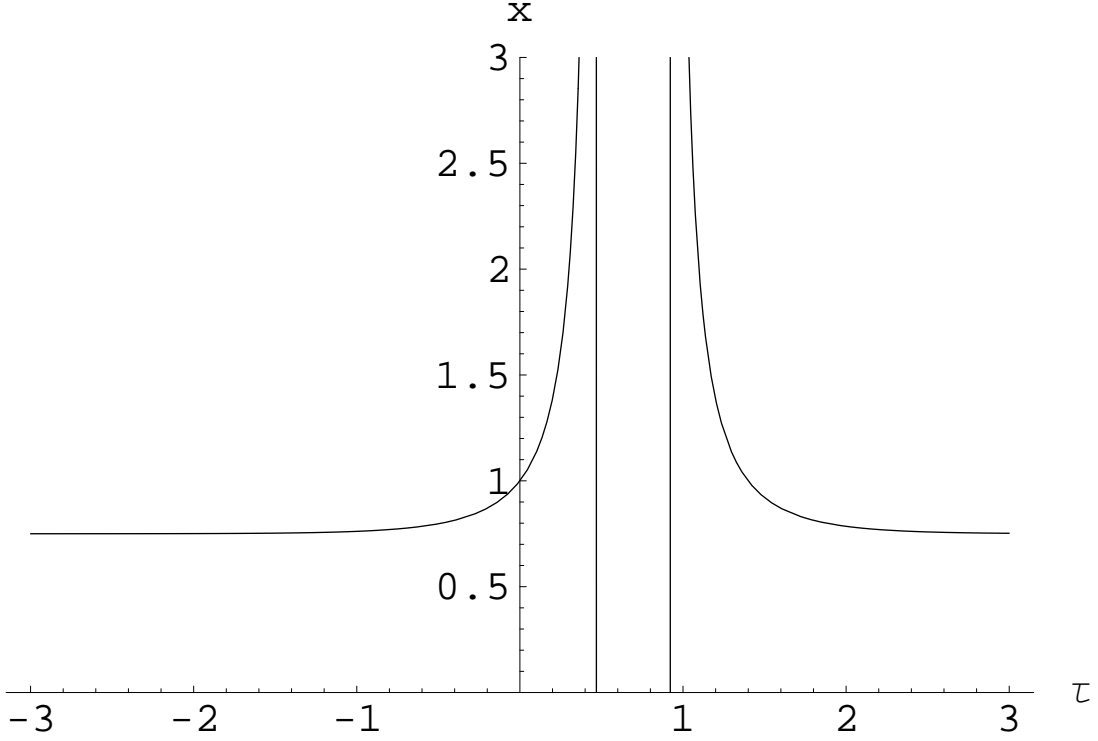


FIG. 9: Only the increasing solution in this figure is physical, it tends to the static solution at minus infinity (both τ and u) and the expansion to infinity takes infinite time (u).

can see that the multiple root must be negative, because of (A3) the simple root must be positive, and thus only the bounce solution can be physical. Again, Fig. 7 applies.

2. $\Omega_{\Lambda,0} < 0$

2.1. $\sigma_6 \neq 0$ – simple roots

As before we obtain a restriction on σ_6

$$\Omega_{k,0} < 0 \Rightarrow \sigma_6 > 0, \quad (\text{A14})$$

and similarly to before, for non-negative curvature any sign is possible. Analyzing the subcases of $\sigma_6 > 0$, we can see that one of the restrictions becomes an identity now. Namely:

$$\Omega_{k,0}^2 + 12\Omega_R\Omega_{\Lambda,0} > 0 \quad (\text{A15})$$

is always true. Furthermore, for $k \leq 0$, we can only have $w_- < 0$, but for $k > 0$ both signs are possible. In consequence, we can have the subcase 2.1.2, which is all the more interesting thanks to (A3), which ensures, that there are oscillations with no singularity; and 2.1.3 with two possible regions of oscillation, also without singularity. They are qualitatively the same as the $\Omega_{\Lambda,0} > 0$ oscillations depicted in Fig. 6.

2.2. $\sigma_6 = 0$ – one double root

Because of (A14), from now on we must have *non-negative curvature*. Obviously, (A11) must still hold, but the intervals of Ω_R are now “reversed”:

$$\frac{16\Omega_R\Omega_{k,0}}{\Omega_{m,0}^2} \in \left(-\infty; -3(3 + \sqrt{3}) \right] \cup \left[-3(3 - \sqrt{3}); 0 \right),$$

finally giving:

$$\frac{16\Omega_R\Omega_{k,0}}{\Omega_{m,0}^2} \in \left[-3(3-\sqrt{3}); 0\right). \quad (\text{A16})$$

Looking at σ_5 as a function of $\Omega_{\Lambda,0}$ with the above restrictions, it is straightforward to check that it can only be negative, thus reducing this case to 2.2.1 only, where only a static, stable solution exists.

2.3. $\sigma_6 = \sigma_5 = 0$, $\sigma_4 \neq 0$ – two double roots

As $\sigma_5 = 0$ has only positive roots with all the current restrictions on the parameters, this and all the further cases are impossible.

-
- [1] A. G. Riess et al. (Supernova Search Team), *Astron. J.* **116**, 1009 (1998), astro-ph/9805201.
[2] S. Perlmutter et al. (Supernova Cosmology Project), *Astrophys. J.* **517**, 565 (1999), astro-ph/9812133.
[3] D. N. Spergel et al. (WMAP), *Astrophys. J. Suppl.* **148**, 175 (2003), astro-ph/0302209.
[4] E. J. Copeland, M. Sami, and S. Tsujikawa, *Int. J. Mod. Phys. D* **15**, 1753 (2006), hep-th/0603057.
[5] T. Padmanabhan, *Phys. Rept.* **380**, 235 (2003), hep-th/0212290.
[6] M. Ishak (2005), astro-ph/0504416.
[7] I. Antoniadis, P. O. Mazur, and E. Mottola, *New J. Phys.* **9**, 11 (2007), gr-qc/0612068.
[8] M. Bordag, U. Mohideen, and V. M. Mostepanenko, *Phys. Rept.* **353**, 1 (2001), quant-ph/0106045.
[9] S. A. Ellingsen and I. Brevik, *J. Phys. A* **40**, 3643 (2007), quant-ph/0611030.
[10] H. B. G. Casimir, *Kon. Ned. Akad. Wetensch. Proc.* **51**, 793 (1948).
[11] K. A. Milton, R. Kantowski, C. Kao, and Y. Wang, *Mod. Phys. Lett. A* **16**, 2281 (2001), hep-ph/0105250.
[12] M. Lachieze-Rey and J.-P. Luminet, *Phys. Rept.* **254**, 135 (1995), gr-qc/9605010.
[13] Y. B. Zeldovich and A. A. Starobinsky, *Sov. Astron. Lett.* **10**, 135 (1984).
[14] M. Szydlowski, J. Szczesny, and M. Biesiada, *Class. Quantum Grav.* **4**, 1731 (1987).
[15] M. Szydlowski and J. Szczesny, *Phys. Rev. D* **38**, 3625 (1988).
[16] M. Szydlowski, J. Szczesny, and T. Stawicki, *Class. Quant. Grav.* **5**, 1097 (1988).
[17] B. McInnes (2006), hep-th/0607074.
[18] V. M. Mostepanenko and N. N. Trunov, *The Casimir Effect and its Applications* (Clarendon Press, Oxford, 1997).
[19] D. Muller (2004), gr-qc/0403086.
[20] W. F. Wreszinski (2006), quant-ph/0603026.
[21] C. A. R. Herdeiro and M. Sampaio, *Class. Quant. Grav.* **23**, 473 (2006), hep-th/0510052.
[22] J. S. Dowker and R. Critchley, *Phys. Rev. D* **15**, 1484 (1977).
[23] E. Streeruwitz, *Phys. Rev. D* **11**, 3378 (1975).
[24] F. W. J. Olver, *Asymptotics and Special Functions* (Academic Press, New York, 1974).
[25] D. J. Mulryne, R. Tavakol, J. E. Lidsey, and G. F. R. Ellis, *Phys. Rev. D* **71**, 123512 (2005), astro-ph/0502589.
[26] W. Godlowski and M. Szydlowski, *Phys. Lett. B* **642**, 13 (2006), astro-ph/0606731.
[27] W. Godlowski, M. Szydlowski, and Z.-H. Zhu (2007), astro-ph/0702237.
[28] C. Molina-Paris and M. Visser, *Phys. Lett. B* **455**, 90 (1999), gr-qc/9810023.
[29] J. D. Barrow, D. Kimberly, and J. Magueijo, *Class. Quant. Grav.* **21**, 4289 (2004), astro-ph/0406369.
[30] P. Singh and A. Toporensky, *Phys. Rev. D* **69**, 104008 (2004), gr-qc/0312110.
[31] Y. V. Shtanov (2000), hep-th/0005193.
[32] Y. Shtanov and V. Sahni, *Class. Quantum Grav.* **19**, L101 (2002), gr-qc/0204040.
[33] V. Sahni and Y. Shtanov, *JCAP* **0311**, 014 (2003), astro-ph/0202346.
[34] Y. Shtanov and V. Sahni, *Phys. Lett. B* **557**, 1 (2003), gr-qc/0208047.
[35] M. Szydlowski, W. Godlowski, A. Krawiec, and J. Golbiak, *Phys. Rev. D* **72**, 063504 (2005), astro-ph/0504464.
[36] A. Borowiec, W. Godlowski, and M. Szydlowski, *Phys. Rev. D* **74**, 043502 (2006), astro-ph/0602526.
[37] A. Borowiec, W. Godlowski, and M. Szydlowski, *Int. J. Geom. Meth. Mod. Phys.* **4**, 183 (2007), astro-ph/0607639.
[38] S. Carloni, P. K. S. Dunsby, and D. M. Solomons, *Class. Quant. Grav.* **23**, 1913 (2006), gr-qc/0510130.
[39] A. G. Riess et al. (Supernova Search Team), *Astrophys. J.* **607**, 665 (2004), astro-ph/0402512.
[40] A. G. Riess et al. (2006), astro-ph/0611572.
[41] P. Astier et al., *Astron. Astrophys.* **447**, 31 (2006), astro-ph/0510447.
[42] R. G. Vishwakarma and P. Singh, *Class. Quant. Grav.* **20**, 2033 (2003), astro-ph/0211285.
[43] R. A. Daly and S. G. Djorgovski, *Astrophys. J.* **597**, 9 (2003), astro-ph/0305197.
[44] Z.-H. Zhu, M.-K. Fujimoto, and X.-T. He, *Astrophys. J.* **603**, 365 (2004), astro-ph/0403228.
[45] D. Puetzfeld, M. Pohl, and Z.-H. Zhu, *Astrophys. J.* **619**, 657 (2005), astro-ph/0407204.
[46] S. Weinberg, *Rev. Mod. Phys.* **61**, 1 (1989).

- [47] R. A. Daly and S. G. Djorgovski, *Astrophys. J.* **612**, 652 (2004), astro-ph/0403664.
- [48] D. J. Eisenstein et al., *Astrophys. J.* **633**, 560 (2005), astro-ph/0501171.
- [49] M. Fairbairn and A. Goobar, *Phys. Lett.* **B642**, 432 (2006), astro-ph/0511029.
- [50] Y. Wang and M. Tegmark, *Phys. Rev. Lett.* **92**, 241302 (2004), astro-ph/0403292.
- [51] V. F. Cardone, C. Tortora, A. Troisi, and S. Capozziello, *Phys. Rev.* **D73**, 043508 (2006), astro-ph/0511528.
- [52] B. K. Tippet and K. Lake (2004), gr-qc/0409088.
- [53] H. Akaike, *IEEE Trans. Auto. Control* **19**, 716 (1974).
- [54] G. Schwarz, *Annals of Statistics* **6**, 461 (1978).
- [55] K. P. Burnham and D. R. Anderson, *Model Selection and Multimodel Inference: A Practical Information – Theoretical Approach* (Springer-Verlag, New York, 2002), 2nd ed.
- [56] A. R. Liddle, *Mon. Not. Roy. Astron. Soc.* **351**, L49 (2004), astro-ph/0401198.
- [57] D. Parkinson, S. Tsujikawa, B. A. Bassett, and L. Amendola, *Phys. Rev.* **D71**, 063524 (2005), astro-ph/0409071.
- [58] W. Godlowski and M. Szydlowski, *Phys. Lett.* **B623**, 10 (2005), astro-ph/0507322.
- [59] M. Szydlowski and W. Godlowski, *Phys. Lett.* **B633**, 427 (2006), astro-ph/0509415.
- [60] M. Szydlowski and W. Godlowski, *Phys. Lett.* **B639**, 5 (2006), astro-ph/0511259.
- [61] M. Szydlowski and A. Kurek (2006), gr-qc/0608098.
- [62] M. Szydlowski, A. Kurek, and A. Krawiec, *Phys. Lett.* **B642**, 171 (2006), astro-ph/0604327.
- [63] A. Kurek and M. Szydlowski (2007), astro-ph/0702484.
- [64] H. Jeffreys, *Theory of Probability* (Oxford University Press, Oxford, 1961), 3rd ed.
- [65] S. Mukherjee, E. D. Feigelson, G. J. Babu, F. Murtagh, C. Fraley, and A. Raftery, *Astrophys. J.* **508**, 314 (1998), astro-ph/9802085.
- [66] P. Mukherjee, D. Parkinson, P. S. Corasaniti, A. R. Liddle, and M. Kunz, *Mon. Not. Roy. Astron. Soc.* **369**, 1725 (2006), astro-ph/0512484.
- [67] R. E. Kass and A. E. Raftery, *J. Amer. Stat. Assoc.* **90**, 773 (1995).
- [68] M. P. Dabrowski and T. Stachowiak, *Annals Phys.* **321**, 771 (2006), hep-th/0411199.